In-vivo validation of spatially correct three-dimensional reconstruction of human coronary arteries by integrating intravascular ultrasound and biplane angiography

George D. Giannoglou[a], Yiannis S. Chatzizisis[a], George Sianos[a], Dimitrios Tsikaderis[b], Antonis Matakos[c], Vassilios Koutkias[d], Panagiotis Diamantopoulos[e], Nicos Maglaveras[d], George E. Parcharidis[a] and George E. Louridas[a]

Objectives **The in-vivo validation of geometrically correct three-dimensional reconstruction of human coronary arteries by integrating intravascular ultrasound and biplane coronary angiography has not been adequately investigated. The purpose of this study was to describe the reconstruction method and investigate its in-vivo feasibility and accuracy.**

Methods **In 17 coronary arteries (mean length, 85.7 ± 17.1 mm) from nine patients, an intravascular ultrasound procedure along with a biplane coronary angiography was performed. From each angiographic projection, a single end-diastolic frame was selected in order to reconstruct the intravascular ultrasound catheter trajectory in space. In each end-diastolic intravascular ultrasound image, the lumen and media–adventitia contours were detected semi-automatically by an active contour algorithm. Each pair of contours was located on the catheter trajectory appropriately and interpolated with the adjacent pairs creating a three-dimensional volume of the arterial lumen and wall. The reconstructed lumen was back-projected onto both angiographic planes and the agreement between the back-projected and the angiographic luminal outlines was calculated.**

Results **The angiogram-derived catheter length showed very high correlation ($y = 0.97x + 1.8$, $P < 0.001$) and agreement with the corresponding pullback-derived values. Accordingly, the semi-automated segmentation of intravascular ultrasound images was also in significant correlation ($r \geq 0.96$, $P < 0.001$) and agreement with the reference manual tracing. The back-projected luminal borders showed good overall association with the corresponding angiographic ones ($r = 0.78$, $P < 0.001$) as well as remarkable agreement.**

Conclusions **Spatially correct three-dimensional reconstruction of human coronary arteries constitutes an imaging method with considerably high in-vivo feasibility and accuracy.** ***Coron Artery Dis*** **17:533–543 © 2006 Lippincott Williams & Wilkins.**

Coronary Artery Disease 2006, **17**:533–543

Keywords: angiography, imaging, three-dimensional, ultrasonics, coronary artery

[a] Cardiovascular Engineering and Atherosclerosis Laboratory, 1st Cardiology Department, AHEPA University Hospital, Aristotle University Medical School, Thessaloniki, Greece, [b]St Luke's Hospital, Thessaloniki Heart Institute, Thessaloniki, Greece, [c]Electrical and Computer Engineering Department, School of Engineering, Aristotle University of Thessaloniki, Thessaloniki, Greece, [d]Laboratory of Medical Informatics, Aristotle University Medical School, Thessaloniki, Greece and [e]Department of Engineering and Design, School of Science and Technology, University of Sussex, Brighton, UK

Correspondence and requests for reprints to Dr Yiannis S. Chatzizisis, MD, MSc, Cardiovascular Engineering and Atherosclerosis Laboratory, 1st Cardiology Department, AHEPA University Hospital, Aristotle University Medical School, 1 St. Kyriakidi Street, 54636 Thessaloniki, Greece
Tel/fax: +30 2310 994837; e-mail: joc@med.auth.gr

Sponsorship: This study has been supported by the Greek State Scholarships Foundation, the Aristotle University Research Committee and the Hellenic Harvard Foundation.

Received 30 November 2005 **Accepted** 28 January 2006

Introduction

Coronary angiography is regarded as the gold standard method for the assessment of severe coronary lesions. It is restricted, however, by its inherent inability to quantify plaque burden beyond the luminal silhouette created by the injected contrast. In the recent years, intravascular ultrasound (IVUS) has been proved to be superior in the imaging of coronary atherosclerosis [1]. IVUS is a catheter-based technique that provides two-dimensional (2D) high-resolution tomographic images of coronary arteries and, therefore, accurate information concerning luminal area, as well as wall thickness and composition. In other words, it provides the most accurate in-vivo estimation of the plaque burden currently available. This estimation is performed by stacking of adjacent 2D images, resulting in linear three-dimensional (3D) vessel volumes, and summating of the plaque areas of the corresponding images in order to determine the extent of

0954-6928

atheroma. This approach, however, ignores the actual vessel curvature and the axial movements of the catheter during the pullback [2], preventing the study of the geometrical and haemodynamic characteristics of the coronary arteries and consequently the investigation of their impact on atherosclerosis.

To overcome the above limitations, a new imaging method was introduced, combining the 3D geometrical information obtained from biplane angiography with the volumetric information derived by IVUS. Initial attempts for the implementation of this method made several significant assumptions concerning the geometrical distortions due to cardiac and respiratory motions, the determination of the spatially correct 3D path of the transducer and the angular twist of the catheter during the pullback, limiting the overall accuracy of the method [3,4]. Although, recent studies [2,5] managed to eliminate the initial assumptions of cardiac motion and catheter's twist by gating IVUS images on electrocardiogram (ECG) and applying rules from differential geometry, respectively, however, the respiratory motion still remains a problem. To date the proposed reconstruction method has been extensively validated in vessel phantoms [2] and *ex vivo* [2,5,6], nevertheless, the human in-vivo accuracy has not been elucidated adequately. In a recent human in-vivo study, the accuracy of the method was examined in 12 stented coronary segments [5]. In particular, the validation was based on the determination of the matching between the reconstructed lumen and the corresponding stent borders identified in angiogram, restricting the accuracy of the method in short arterial segments. However, the human in-vivo reliability of the method in longer coronary segments, using the angiographic luminal outlines, instead of stent outlines as a measure of agreement has not been investigated yet.

The purpose of this study was to present the method for the geometrically correct 3D reconstruction of human coronary arteries based on integration of IVUS and biplane angiography as well as to determine its in-vivo feasibility and accuracy in a representative data set including long arterial segments.

Methods

Study population

In all, 17 arterial segments [right coronary artery (RCA), $n = 7$; left anterior descending (LAD), $n = 3$; left circumflex artery (LCx) $n = 6$; first diagonal branch (D_1), $n = 1$] derived from nine patients were investigated. All patients were randomly selected during routine diagnostic and therapeutic interventional procedures. The examined coronary arteries – more than one in some patients – were included in the study regardless of the extent of their lesions, varying from minimal to severe. The clinical and angiographic characteristics of the study population are presented in Table 1. The study protocol was approved by the Institutional Medical Ethics Committee and written informed consent was obtained from all participants.

Table 1 Clinical and angiographic characteristics of the study population

Clinical characteristics of patients ($n=9$)	
Age (years), mean ± SD	58.3 ± 10.8
Sex, male	6
Hypertension	6
Diabetes	0
Dyslipidemia	5
Smoking	4
Family history	2
Angina	8
Previous MI	3
Previous PTCA	4
CABG	1
SBP (mmHg), mean ± SD	132 ± 26
DBP (mmHg), mean ± SD	70 ± 22
Angiographic characteristics of arteries ($n=17$)	
Target vessel	17
RCA	7
LAD	3
LCx	6
D_1	1
Angiography only	9
PTCA with stent	8
DES	7
Non-DES	1

MI, myocardial infarction; PTCA, percutaneous transluminal coronary angioplasty; CABG, coronary artery by-pass graft; SBP, systolic blood pressure; DBP, diastolic blood pressure; RCA, right coronary artery; LAD, left anterior descending; LCx, left circumflex; D_1, first diagonal branch; DES, drug-eluting stent.

Biplane angiogram acquisition and pre-processing

The principal steps of the entire method are schematically presented in Fig. 1. Initially, the IVUS catheter was inserted through a 6 F guiding catheter into the investigated coronary artery. With the catheter at its most distal location, a biplane coronary angiogram was recorded (Siemens Medical Solutions A.G., Forchheim, Germany; Philips Medical Systems B.V., Eindhoven, The Netherlands). In order to secure better imaging resolution, the utilized angiographic projections were set to be orthogonal, preferably at right anterior oblique (RAO) 30° and left anterior oblique (LAO) 60°, with zero cranial or caudal orientation. All the biplane angiograms, along with the ECG for synchronization, were recorded in DICOM format at a rate of 12.5 frames/s and image size of 512×512 pixels with 8-bits grey scale.

From each angiographic projection, a single end-diastolic frame was selected corresponding to the peak of R-wave on ECG. With a quantitative coronary angiography software package (CAAS II; Pie Medical Imaging, Maastricht, The Netherlands), the luminal outlines were detected semi-automatically in each selected frame. For conversion of pixel size to its actual size in millimeters, the scaling factor was determined in each projection, using the 6 F guiding catheter as reference.

Fig. 1

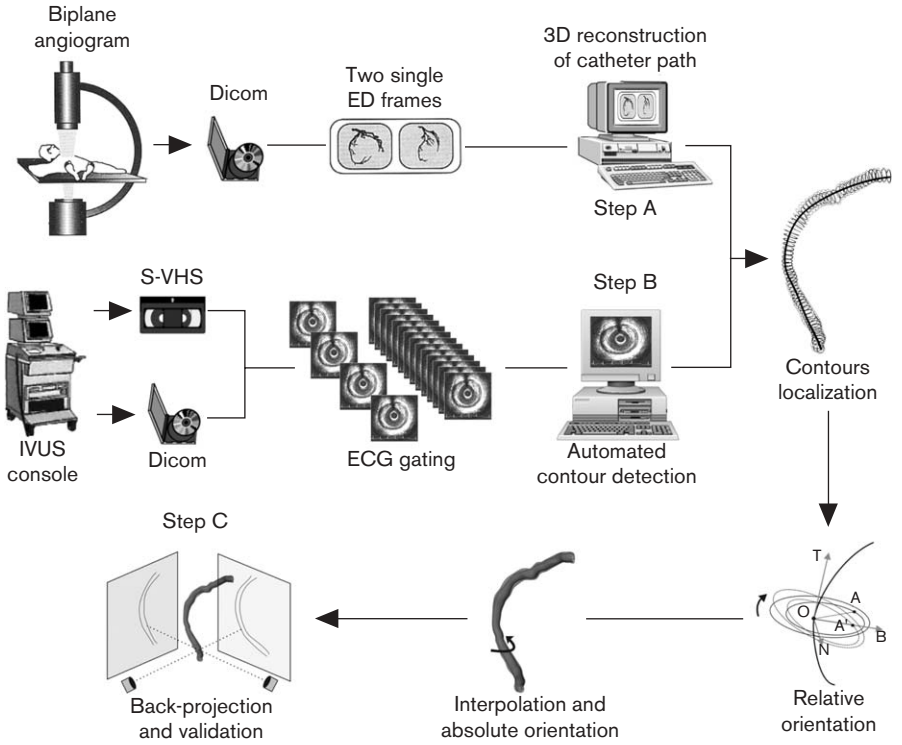

The principal steps of the three-dimensional (3D) reconstruction method of coronary arteries based on fusion of data from intravascular ultrasound (IVUS) and biplane angiography. From each angiographic projection, a single end-diastolic (ED) frame was selected in order to reconstruct the IVUS catheter path in space (step A). The IVUS images were digitized and gated to the electrocardiogram (ECG) for the selection of end-diastolic images. In each end-diastolic image, the lumen and media–adventitia contours were detected semi-automatically by an active contour algorithm (step B). Each pair of contours was located onto the catheter path and orientated in space appropriately. The correctly orientated luminal and media–adventitia contours were interpolated with additional intermediate contours, generating a 3D lumen and vessel volume, respectively. To determine the spatially correct orientation of the reconstructed vessel, the reconstructed lumen was back-projected onto each angiographic plane and rotated iteratively searching for the best possible match with the corresponding angiographic luminal edges. The agreement between the back-projected and the angiographic luminal outlines was calculated in order to find the overall accuracy of the method (step C).

Catheter path three-dimensional reconstruction

To reconstruct the correct catheter 3D path [7], the IVUS catheter was delineated from the tip of the transducer up to the outlet of the guiding catheter in each projection. The resultant 2D curves were extracted vertically to their angiographic planes and intersected with each other creating a 3D curve that corresponded to the geometrically correct IVUS catheter 3D path (Fig. 2).

Intravascular ultrasound acquisition and pre-processing

IVUS was performed with a mechanical imaging system (ClearView; Boston Scientific, Natick, Massachusetts, USA) and a 2.6 F sheath-based catheter, incorporating a 40 MHz single-element transducer rotating at 1800 rpm and yielding 30 images/s (Atlantis SR Pro; Boston Scientific). A motorized pullback device was applied to withdraw the catheter from its most distal point to the outlet of the guiding catheter at a constant speed of 0.5 mm/s. All ultrasound data, along with the simultaneous ECG, were recorded in 0.5-inch S-VHS videotape. The S-VHS data was digitized by a frame-grabber at 512×512 pixels with 8-bit grey scale at a rate of 7.5 images/s, and the end-diastolic images were selected. The 1-mm distance markers in the original IVUS images were used for pixel size calibration. From each image, a 340×340 pixels sub-image was extracted, including the region of interest and the transducer of the catheter in the centre of the image. In the resulting frame sequence, an unsharpened mask filter was applied to augment the luminal and media–adventitia leading edges compensating for noise.

Segmentation of intravascular ultrasound images

The lumen and media–adventitia borders [1] were detected semi-automatically in the sequence of the end-diastolic IVUS images by a custom-developed computer algorithm based on active contour models, also known as snakes [8,9]. The first step of the segmentation algorithm included the consecutive initialization of two

Fig. 2

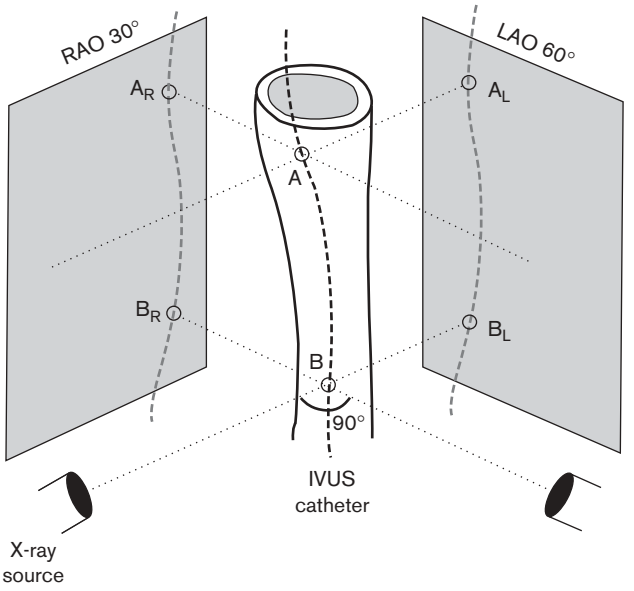

Schematic presentation of the orthogonal biplane angiographic imaging system. 'B' and 'A' depict the pullback start and end, respectively. B_R, A_R and B_L, A_L correspond to the projection of 'B' and 'A' on the right anterior oblique (RAO) and left anterior oblique (LAO) angiographic plane, respectively. IVUS, intravascular ultrasound.

snakes in the first image by providing manually two initial closed contours, roughly near the luminal and media–adventitia boundaries, respectively. Afterwards, the detection algorithm was launched and both snakes were deformed automatically by minimizing their energy function to capture the corresponding boundaries. In case the result was not satisfactory, the user could either re-initialize the snakes and launch the detection mechanism again or interactively calibrate the algorithm by adjusting several parameters appropriately [8]. Upon satisfactory segmentation in the first image, the algorithm was applied automatically in the second image, using the detected contours of the first image as the initialization scheme. The same process was repeated for the rest of the images of the sequence. The user could review the final output and, if it was not the optimal one in part of the image sequence, the above process was iterated, starting from the image in which the detected boundary diverged from the actual one.

Contour positioning and relative orientation

All pairs of contours (luminal and media–adventitia) were assigned equidistantly and perpendicularly onto the reconstructed catheter path. As an angular rotation of the IVUS catheter during pullback could distort the real geometry of the reconstructed artery, the correct rotational orientation of the luminal contours [2] was determined by implementing a custom-developed algorithm based on Frenet–Serret theorem (see Appendix for details).

Absolute orientation

The correctly orientated luminal and media–adventitia contours were interpolated with additional intermediate contours, generating a 3D volume of lumen and wall, respectively. To determine the spatially correct orientation of the reconstructed vessel, the interpolated lumen was rotated iteratively searching for the best possible match with the corresponding angiographic luminal edges. This was accomplished by back-projecting the reconstructed lumen onto each angiographic plane and comparing the projected luminal borders with the angiographic ones by a custom-developed automated algorithm. The correlation coefficients between these borders were calculated for each angle of rotation, and the angle with the maximum correlation coefficient determined the best match and consequently the absolute orientation of the reconstructed artery.

Validation of three-dimensional path reconstruction method

Despite the absence of any standard method for the objective evaluation of our method, an indirect evaluation could be performed regarding three significant parts of the technique, namely the 3D reconstruction of catheter path (Fig. 1, step A), the segmentation of IVUS images (Fig. 1, step B) and the establishment of absolute orientation of the reconstructed lumen (Fig. 1, step C).

To examine the accuracy of the 3D reconstruction of the catheter path, the length of the reconstructed path (L_{angio}) from its most distal position up to the guiding catheter was compared with its actual length (L_{IVUS}) calculated by the known pullback parameters, according to the following equation:

$$L_{\text{IVUS}} = \frac{\text{total frames}}{\text{frame rate}} \text{pullback velocity},$$

where the pullback velocity was 0.5 mm/s and the frame rate was 7.5 images/s.

Validation of segmentation algorithm

The intra-observer correlation (IOC), which constitutes a measurement of reproducibility, and the inter-observer correlation (INC) of semi-automated segmentation were investigated by two independent experts in 50 randomly selected images. Each image was traced manually, according to the accepted international standards [1], by both experts initially and after a month. Similarly, the same images were segmented semi-automatically by both experts initially and only by the first expert a month apart. Thus, in total, four manual and three semi-automated segmentations were performed in each image. The parameters used for the calculation of IOC and INC were lumen cross-sectional area (LCSA, mm^2), vessel

cross-sectional area (VCSA, mm^2), maximum lumen diameter (MLD, mm) and maximum vessel diameter (MVD, mm). Additionally, the IOC and INC of semi-automated tracing were evaluated for lumen (LV, mm^3), vessel (VV, mm^3) and wall volume (WV, mm^3) in five randomly selected pullbacks.

To assess the accuracy of the semi-automated algorithm, the semi-automatically determined borders compared with the reference manual tracing, using the cross-sectional areas (LCSA and VCSA; $n = 50$) and the maximum diameters (MLD and MVD; $n = 50$) as compared parameters. The sample of 50 images was considered adequate for the reliability of the method comparison study [10]. The average of the above parameters between the initial manual segmentations of both experts was considered as a reference value.

Finally, for the temporal evaluation of the methods, the mean duration of manual ($n = 4$) and semi-automated tracings ($n = 3$) were compared to each other.

Overall method validation

Provided that the output of our method was a 3D reconstructed lumen along with the wall, the quantitative and qualitative detection of high agreement between the reconstructed lumen back-projected onto each angiographic plane and the corresponding angiographic lumen would be a very effective measure of accuracy for the entire technique.

The quantitative validation was implemented in Matlab (The MathWorks Inc., Natick, Massachusetts, USA) by calculating the matching between the back-projected and angiographic lumen; the latter used as reference. The point at which the plane of each frame was intersected with the path of the catheter was considered to be the control point (grey dot in Fig. 3). In each angiographic view, the distances between the catheter path and the angiographic luminal outlines (Z_1 and Z_2) were measured at each control point and considered as random variable X (Fig. 3). Then, the entire set of contours was rotated consecutively by 2° to complete a full circle (180 rotations). For each angle of rotation, the reconstructed lumen was back-projected onto the RAO 30° and LAO 60° plane and the corresponding distances between the catheter path and the projected luminal edges (S_1 and S_2) were calculated, thus creating random variables Y_i ($i = 1,\ldots,180$) (Fig. 3). These distances were compared with each other (Z_1 vs. S_1 and Z_2 vs. S_2 at RAO 30° and Z_1 vs. S_1 and Z_2 vs. S_2 at LAO 60°) resulting in four comparisons for each rotational angle at each control point. The correlation coefficients between the variables X and Y_i were measured and the angle with the maximum correlation coefficient determined the best possible match between the angiographic and back-projected lumen in both projections.

Fig. 3

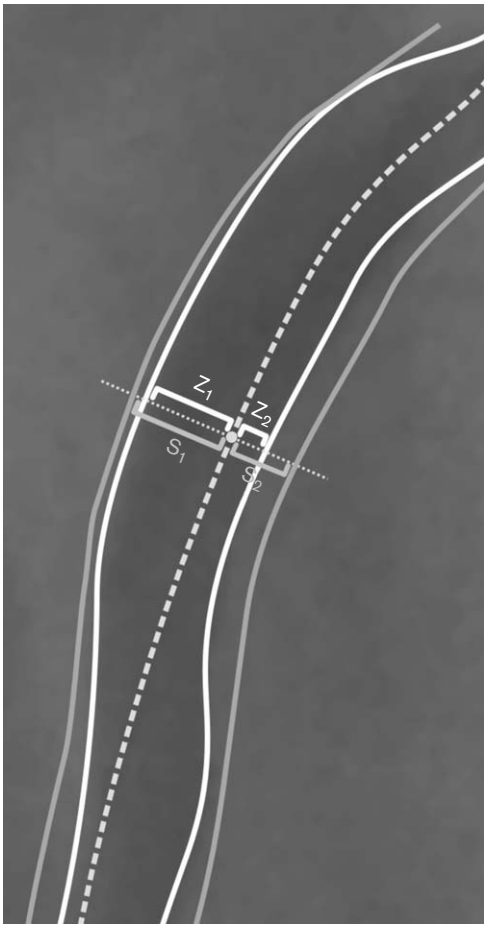

Overall validation of the reconstruction method in a right coronary artery segment. The intravascular ultrasound catheter is depicted with the grey dashed line, while the white and grey solid lines correspond to the angiographic and back-projected luminal outlines, respectively. At each control point (grey dot), the angiographic distances (Z_1 and Z_2) were compared with the corresponding back-projected ones (S_1 and S_2).

Accordingly, to examine how well the shape of the reconstructed lumen fitted the actual angiographic one, the angiographic luminal diameters ($Z = Z_1 + Z_2$) and the back-projected ones ($S = S_1 + S_2$) were correlated at each control point in each projection (Fig. 3). Thus, two comparisons at each control point for every rotational angle were made (Z vs. S).

In order to determine the overall quantitative agreement of the method, all the distances and diameters of the 17 reconstructed lumens were concentrated in a data pool and compared with the corresponding values of the angiographic lumens.

For the qualitative evaluation of the reconstruction method each correctly orientated reconstructed lumen

Fig. 4

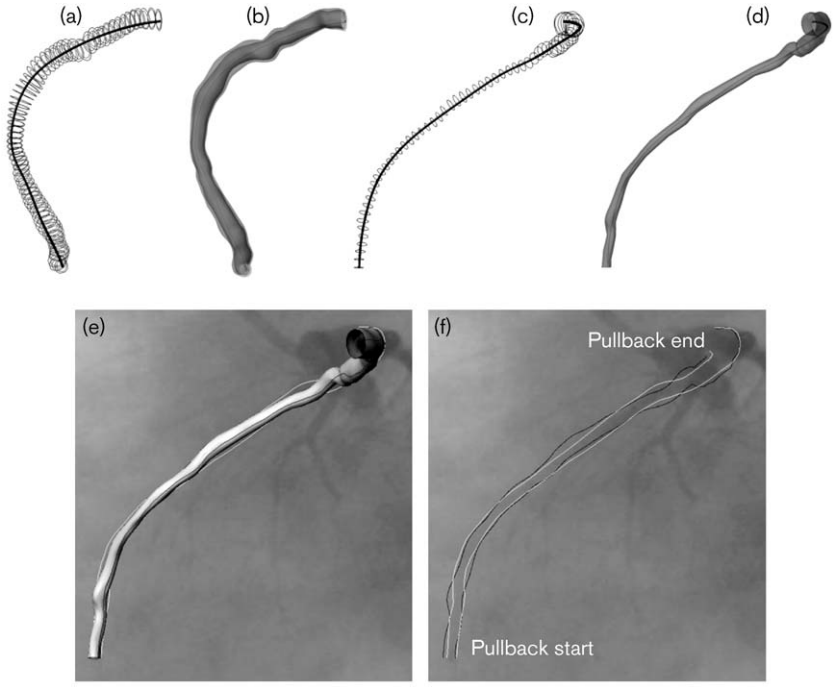

(a) A three-dimensional (3D) reconstructed right coronary artery (RCA) segment with the luminal end media–adventitia contours correctly orientated in space. (b) Transparent view of the reconstructed RCA lumen along with the wall. The intravascular ultrasound catheter is also depicted. (c) The luminal contours of a left anterior descending (LAD) segment. (d) The corresponding 3D reconstruction of the LAD lumen. (e) The LAO 60° angiogram of the LAD and the corresponding reconstructed lumen back-projected on it. (f) The angiographic and back-projected luminal outlines of the same vessel are delineated with white and black lines, respectively, yielding a satisfactory matching.

was back-projected and compared visually with the corresponding angiographic luminal edges.

Statistical analyses

The IOC and INC of the semi-automated segmentation were investigated by linear regression analysis and the Pearson's product–moment correlation coefficient. The comparisons of the semi-automated contour detection with the reference manual were studied with the Bland–Altman analysis. Bland–Altman and linear regression analysis were also used for the comparison between the pullback-derived and angiogram-derived length of the catheter. Provided that both distances and diameters did not fulfil the assumption of normality, which is quite common in large samples, the agreement between the reconstructed lumen and the corresponding angiographic outlines was examined with the Spearman's correlation coefficient and the Bland–Altman analysis. Finally, for the temporal comparison between manual and semi-automated tracing, the two-tailed Student's *t*-test for unpaired data was performed.

All statistical analyses were performed by SPSS, version 12.0 (SPSS Inc., Chicago, Illinois, USA). Data are presented as means ± SD and $P < 0.05$ was considered as the level of significance.

Results

The 3D reconstruction method was successfully implemented in all the examined coronary arteries ($n = 17$) regardless of the severity of the lesions. Figure 4 illustrates a reconstructed RCA and LAD segment. For each artery, 1286 ± 257 (range, 809–1653) IVUS images were recorded, from which 199 ± 52 (range, 126–287) end-diastolic images were selected.

Catheter path reconstruction

The mean length of the reconstructed catheters (L_{IVUS}), calculated from the known pullback parameters, was 85.7 ± 17.1 mm (range, 53.9–110.2 mm, $n = 17$), while the corresponding angiogram-derived value was 85.3 ± 16.8 mm (range, 55.7–109.1 mm, $n = 17$). With Bland–Altman analysis, the L_{angio} showed remarkably high agreement with the reference L_{IVUS}. In particular, the mean difference between L_{IVUS} and L_{angio} was 0.44 mm, while all the differences were concentrated within the limits of agreement (from −3.97 to 4.85 mm) (Fig. 5a). Additionally, L_{IVUS} and L_{angio} revealed high

Fig. 5

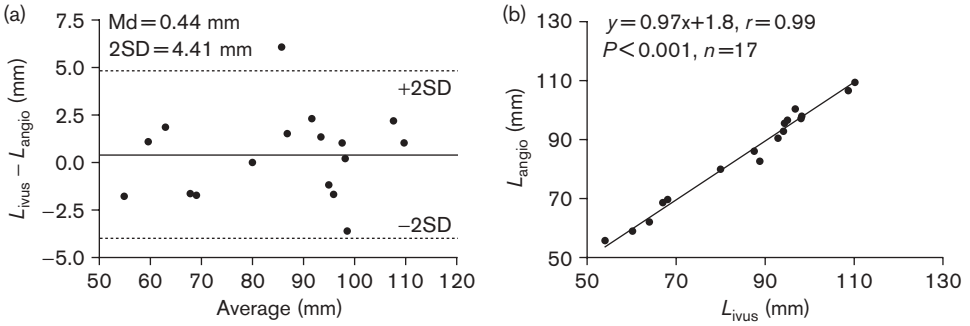

Graphs illustrate the comparison between pullback-derived and angiogram-derived catheter length. (a) Bland–Altman plot of differences against average. The mean difference (Md) and the limits of agreement (±2SD) are indicated with solid and dotted lines, respectively. (b) Linear regression analysis.

Fig. 6

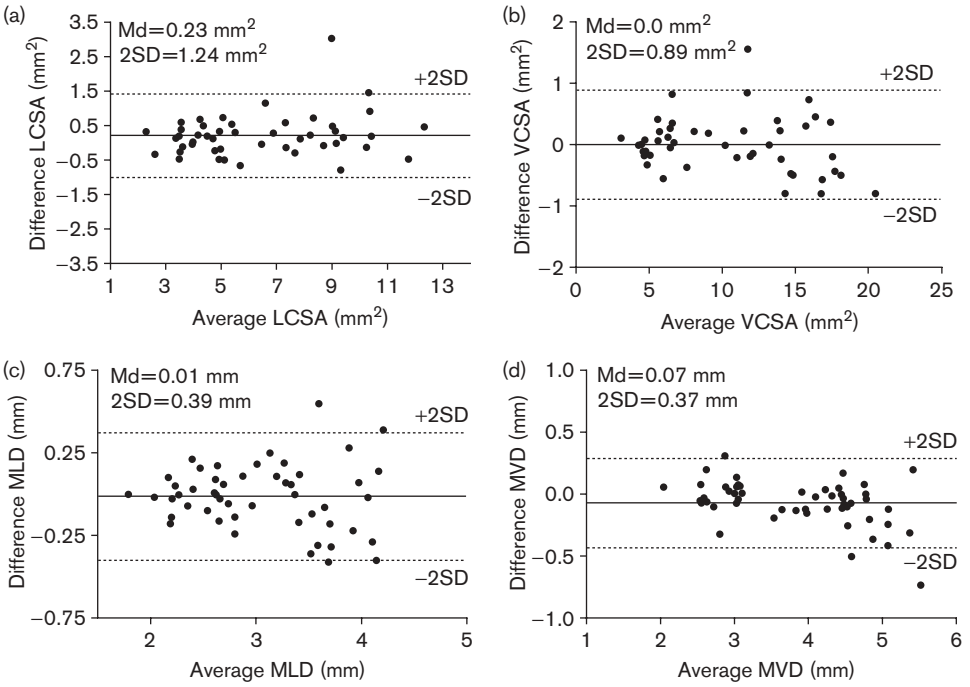

Graphs illustrate Bland–Altman plots of differences between manual and semi-automated segmentation against their average for (a) lumen cross-sectional area (LCSA), (b) vessel cross-sectional area (VCSA), (c) maximum lumen diameter (MLD), and (d) maximum vessel diameter (MVD).

correlation in linear regression analysis ($y = 0.97x + 1.8$, $r = 0.99$, $P < 0.001$, $n = 17$), in which the slope and intercept values were close to 1 and 0, respectively (Fig. 5b).

Intravascular ultrasound image segmentation

The semi-automated segmentation showed significantly high IOC ($r \geq 0.97$) and INC ($r \geq 0.95$) for areas (LCSA, VCSA) and maximum diameters (MLD, MVD) ($P < 0.01$, $n = 50$). Accordingly, the IOC and INC of the segmentation algorithm for all the volumetric parameters (LV, VV, WV) were high ($r \geq 0.95$, $P < 0.01$, $n = 5$). The Bland–Altman plots of differences between semi-automated and manual tracing against their average, revealed that the proposed method had minor differences as compared with the reference manual for all the

Fig. 7

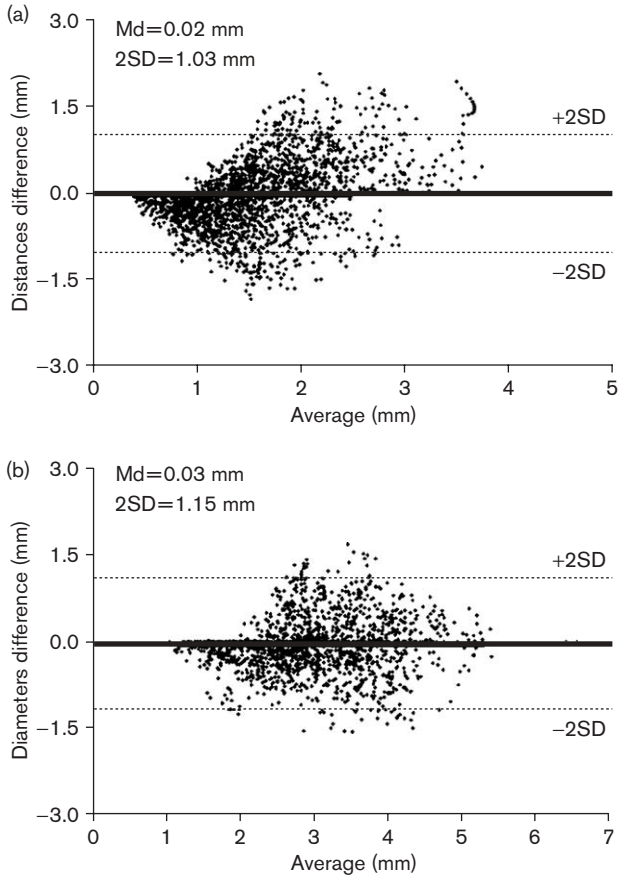

Graphs illustrate Bland–Altman plots of differences between the back-projected and angiographic luminal outlines against their average for (a) distances and (b) diameters.

calculated parameters (Fig. 6a–d). Likewise, linear regression analysis and the corresponding Pearson's correlation coefficients showed that the semi-automated algorithm correlated well with the reference manual and yielded the equations $y = 0.93x + 0.22$, $r = 0.97$ and $y = 1.01x - 0.14$, $r = 0.99$ for LCSA and VCSA, respectively ($P < 0.001$, $n = 50$). Similarly, the corresponding equations for MLD and MVD were $y = 0.98x + 0.07$, $r = 0.96$ and $y = 1.07x - 0.2$, $r = 0.99$, respectively ($P < 0.001$, $n = 50$). It is noteworthy that in the above equations the values of slope and intercept were close to 1 and 0, respectively.

The average analysis time for manual and semi-automated segmentation was reduced significantly by 76.2% (1.43 min/image for manual segmentation vs. 0.34 min/image for semi-automated segmentation, $P = 0.001$, $n = 7$).

Three-dimensional reconstruction method

On average, 57.3 ± 10.7 (range, 40–80) control points were assigned in each coronary artery. Totally, 3896 and 1948 comparisons were made for distances and diameters, respectively, for every rotational angle. As the above values were not distributed normally, the Spearman's correlation coefficient was calculated. At the best-fit angle, an average correlation coefficient of 0.78 for distances and 0.85 for diameters was revealed for all the reconstructed arteries ($P < 0.001$). Bland–Altman plots of differences between the actual and back-projected luminal borders against their means for distances and diameters showed that our method was in good agreement with the reference angiograms. Specifically, the mean difference was −0.02 mm for distances (Fig. 7a) and −0.03 mm for diameters (Fig. 7b), while the great majority of the differences was included within the limits of agreement (from −1.05 to 1.01 mm and from −1.18 to 1.12 mm, respectively). Visually, the back-projected and the actual lumen in each projection revealed good agreement (Fig. 4f).

Discussion

In this study, we implemented and validated an imaging technique for the in-vivo geometrically correct 3D reconstruction of human coronary arteries by integration of IVUS and biplane angiography. The angiographic data provided information about the spatial trajectory of the IVUS catheter, served as the 'backbone', on which the 2D vessel tomographic images from IVUS were positioned and orientated in space. For the in-vivo validation of this method, each reconstructed lumen was back-projected onto both angiographic planes and compared quantitatively with the angiographic luminal outlines. Although the reconstruction method has been validated extensively in vessel phantoms [2] and *ex vivo* [2,5,6] revealing high accuracy, nonetheless, the human in-vivo reliability has not been adequately investigated. The only human in-vivo study existing in the literature has investigated the method's accuracy in 12 coronary arteries; however, the validation was restricted in rather short arterial segments including stents [5]. Therefore, further in-vivo investigation in a larger representative data set, including longer arterial segments and using the luminal outlines, instead of stent borders, as a measure of agreement between the reconstructed lumen and the actual angiographic outlines was needed. In the present study, the in-vivo validation was accomplished in 17 long arterial segments with an average length of 85.7 ± 17.1 mm and the accuracy was found to be significantly high. Besides the high accuracy, the method was found elsewhere to have high in-vivo reproducibility [11].

Several problems arose during the implementation of the method; namely, the twisting motion of the IVUS catheter during the pullback and the geometrical

distortions due to cardiac and respiratory movements. The relative error from the catheter's twist was corrected by the implementation of a custom-developed algorithm based on Frenet–Serret rules, while the geometrical inaccuracies due to cardiac motion were eliminated by gating of IVUS images on the ECG. Although, in this study, the gating was performed manually, the application of new ECG-triggering devices could significantly reduce the analysis time [5]. As far as the respiratory motion was concerned, it still remains a problem, despite the fact that the patients were advised to stop breathing for 3–5 s during the pre-pullback angiogram recording.

Three-dimensional catheter path reconstruction

To reconstruct in space the catheter path, an easily applicable computer algorithm was used based on the fusion of the detected 2D paths in each angiographic projection. The accuracy of this algorithm was assessed by comparing the length of the reconstructed path with the actual length derived from the pullback and was found to be significantly high in both Bland–Altman and linear regression analysis ($y = 0.97x + 1.8$).

To date, two different approaches have been developed for the 3D reconstruction of the catheter trajectory. The first, which is applied in our study, included the acquisition of two pre-pullback angiographic frames from different angles, preferably orthogonal and a fusion of them. This approach is restricted in the application of sheathed catheters only, which pre-define the pullback course of the IVUS transducer [2,5]. The main advantage of this method is the elimination of the respiration-induced geometrical distortions. According to the second approach, the IVUS transducer is followed in time and space during the pullback and the consecutive locations of the transducer are recorded continuously by a biplane angiographic system and interpolated appropriately [6,12]. The in-vivo application of this methodology, however, remains challenging because of the cardiac and respiratory motion and high-radiation exposure [13]. Our future work includes the development of a new imaging system, in which the IVUS transducer will be tracked in space by a radiofrequency positioning sensor avoiding the performance of coronary angiography.

Segmentation algorithm

In this study, a semi-automated method for lumen and media–adventitia border detection in sequential IVUS images was introduced, providing an added value in the method and at the same time substantially decreasing the required analysis time. This technique was based on active contours and showed high feasibility providing satisfactory border detection even in bad-quality images with either artefacts (e.g. the shadowing effect by calcified plaques) or gaps (e.g. in case of branches). The proposed algorithm yielded significantly high agreement with the reference manual contour detection as well as high IOC and INC. These results are comparable to others reported in the literature [14].

Absolute orientation

The absolute orientation of the entire set of frames was determined with iterative back-projections of the reconstructed lumen onto both angiograms and searching for the best-fit angle. The determination of absolute orientation was also used as a measure of how well the reconstructed lumen fitted the actual one in angiograms, by calculating the correlation coefficients for distances and diameters. The correlation coefficient for distances indicated the overlap between the back-projected and the actual lumen, while the correlation coefficient for diameters was used as a measure of how well the back-projected and actual lumen fitted in shape and size [6]. Comparing the reconstructed lumen with the angiographic outlines, the correlation coefficient was found to be 0.78 and 0.85 for distances and diameters, respectively. In a similar in-vivo study [5], the corresponding values were 0.92 and 0.92; however, as mentioned, in that study the matching between the back-projected and the actual lumen was based on stent borders. In the same study, when the luminal borders were used as the matching criterion, instead of stent borders, the correlation coefficient for distances reduced to 0.84, which was comparable to our results ($r = 0.78$). Despite the fact that the stent-based validation revealed better matching, the validation based on lumen borders is considered to be a more realistic approach. In addition, the lumen-based determination of absolute orientation permits the reconstruction of longer arterial segments, even without stent.

Ideally, the back-projected luminal borders should be in perfect agreement with the actual angiographic ones. The divergence found in our study was attributed to several factors; namely, the vessel foreshortening and the difficulty in detecting the IVUS catheter and the luminal edges in angiograms with absolute accuracy, due to their inherent poor imaging resolution [6].

Study limitations

Several limitations exist in this study. First, the applicability of our method was limited to IVUS imaging systems utilizing sheath-based catheters, which secure a steady pullback trajectory. Furthermore, in order to reduce the analysis time, we assigned the lumen and media-adventitia contours equidistantly on the catheter path, although it would be more accurate to place each one at a specific location, calculated from its known identical number, pullback velocity and frame rate [2]. Nevertheless, the equidistant approach has been applied elsewhere without compromising the overall accuracy [5]. Although the pullback-derived catheter length was considered as a reference value in order to evaluate the catheter 3D reconstruction algorithm, the fact that,

theoretically, the catheter sometimes might delay during the pullback could potentially influence the reference length. In our study, however, no significant pullback retardations were noticed. The total duration of the method from data acquisition till the time when a complete 3D rendering was on the computer screen was approximately 2.5–3 h. This could be significantly reduced to half or even more than that, by applying an ECG-triggering device and a fully-automated IVUS segmentation algorithm.

Conclusions and clinical perspectives

The spatially correct 3D reconstruction of human coronary by integrating IVUS and biplane angiography constitutes an imaging method with a markedly high in-vivo feasibility and accuracy regardless of the severity of coronary lesions. This asset makes the method a valuable diagnostic and research tool. In particular, this technique could facilitate rapid and more reliable, compared with the conventional straight 3D reconstructions, plaque morphometric analyses (planimetry, volumetric measurements, wall thickness and plaque eccentricity calculations), improving the clinical decision-making and stent-positioning quality [13]. In addition, it might enable interactive exploration of interior arterial structures by fly-through or cut-off views alleviating the restrictions of angiography associated with viewing from limited angles. Furthermore, it could be used in the customized planning of intracoronary brachytherapy [12].

As far as its potential investigational utility is concerned, the method might be used for the evaluation of the impact of pharmaceutical or mechanical (e.g. stent) interventions on plaque progression and regression through follow-up studies [13,15]. It is also anticipated to facilitate the estimation of 3D geometry and the application of computational fluid dynamics simulations in order to study the effect of geometrical (e.g. curvature, torsion) [16] or haemodynamic factors (e.g. shear stress) [15] on atherogenesis and plaque progression.

Future work will focus on the development of an integrated application, which through a user-friendly graphical interface is anticipated to provide online diagnostic and therapeutic support to the invasive cardiologist.

Acknowledgement

The authors would like to thank Ms Chrysanthi Basdekidou for her contribution to ECG gating of IVUS images.

References

1 Mintz GS, Nissen SE, Anderson WD, Bailey SR, Erbel R, Fitzgerald PJ, *et al.* American college of cardiology clinical expert consensus document on standards for acquisition, measurement and reporting of intravascular ultrasound studies (IVUS). A report of the American College of Cardiology Task Force on clinical expert consensus documents. *J Am Coll Cardiol* 2001; **37**:1478–1492.
2 Wahle A, Prause GPM, DeJong SC, Sonka M. Geometrically correct 3-D reconstruction of intravascular ultrasound images by fusion with biplane angiography: methods and validation. *IEEE Trans Med Imaging* 1999; **18**:686–699.
3 Evans JL, Ng KH, Wiet SG, Vonesh MJ, Burns WB, Radvany MG, *et al.* Accurate three-dimensional reconstruction of intravascular ultrasound data. Spatially correct three-dimensional reconstructions. *Circulation* 1996; **93**:567–576.
4 Pellot C, Bloch I, Herment A, Sureda F. An attempt to 3D reconstruct vessel morphology from X-ray projections and intravascular ultrasounds modeling and fusion. *Comp Med Imaging Graph* 1996; **20**:141–151.
5 Slager CJ, Wentzel JJ, Schuurbiers JCH, Oomen JAF, Kloet J, Krams R, *et al.* True 3-dimensional reconstruction of coronary arteries in patients by fusion of angiography and IVUS (ANGUS) and its quantitative validation. *Circulation* 2000; **102**:511–516.
6 Cothren R, Shekhar R, Tuzcu M, Nissen S, Cornhill F, Vince G. Three-dimensional reconstruction of the coronary artery wall by image fusion of intravascular ultrasound and biplane angiography. *Int J Cardiol Imaging* 2000; **16**:69–85.
7 Chatzizisis YS. Three-dimensional reconstruction of coronary arteries by fusion of intravascular ultrasound and biplane angiography. MSc Dissertation. Thessaloniki, Greece: Aristotle University Medical School; 2004.
8 Kass M, Witkin A, Terzopoulos D. Snakes: active contour models. *Int J Comp Vision* 1987; **1**:321–331.
9 Kompatsiaris I, Tzovaras D, Koutkias V, Strintzis MG. Deformable boundary detection of stents in angiographic images. *IEEE Trans Med Imaging* 2000; **19**:652–662.
10 Bland JM, Altman DG. Statistical methods for assessing agreement between two methods of clinical measurement. *Lancet* 1986; **1**:307–310.
11 Coskun AU, Yeghiazarians Y, Kinlay S, Clark ME, Ilgebusi OJ, Wahle A, *et al.* Reproducibility of coronary lumen, plaque, and vessel wall reconstruction and of endothelial shear stress measurements in vivo in humans. *Catheter Cardiovasc Interv* 2003; **60**:67–78.
12 Weichert F, Muller H, Quast U, Kraushaar A, Spilles P, Heintz M, *et al.* Virtual 3D IVUS vessel model for intravascular brachytherapy planning. I. 3D segmentation, reconstruction, and visualization of coronary artery architecture and orientation. *Med Phys* 2003; **30**:2530–2536.
13 Klingensmith JD, Schoenhagen P, Tajaddini A, Halliburton SS, Tuzcu M, Nissen SE, *et al.* Automated three-dimensional assessment of coronary artery anatomy with intravascular ultrasound scanning. *Am Heart J* 2003; **145**:795–805.
14 Kovalski G, Beyar R, Shofti R, Azhari H. Three-dimensional automated quantitative analysis of intravascular ultrasound images. *Ultrasound Med Biol* 2000; **26**:527–537.
15 Stone PH, Coskun AU, Kinlay S, Clark ME, Sonka M, Wahle A, *et al.* Effect of endothelial shear stress on the progression of coronary artery disease, vascular remodeling and in-stent restenosis in humans. *Circulation* 2003; **108**:438–444.
16 Krams R, Wentzel JJ, Oomen JA, Vinke R, Schuurbiers JCH, de Feyter PJ, *et al.* Evaluation of endothelial shear stress and 3D geometry as factors determining the development of atherosclerosis and remodeling in human coronary arteries in vivo. Combining 3D reconstruction from angiography and IVUS (ANGUS) with computational fluid dynamics. *Arterioscler Thromb Vasc Biol* 1997; **17**:2061–2065.
17 Millman RS, Parker GD. *Elements of differential geometry.* New Jersey: Prentice-Hall; 1997.

Appendix

According to the Frenet–Serret theorem [2,17], if a parameterized space curve is known, an orthonormal basis consisting of three vectors, namely the tangent (T), normal (N) and binormal (B), can be evaluated (Fig. 8). These vectors define a reference frame (Frenet frame or moving trihedron), which moves tangentially to the curve.

Fig. 8

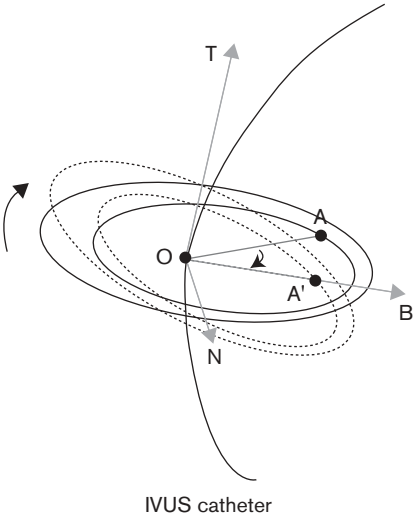

Schematic presentation of the Frenet–Serret moving trihedron defined by the vectors T (tangent), N (normal) and B (binormal). The depicted pair of contours (solid lines) was rotated around the control point (O) at the plane defined by N and B, so as the initial reference axis (OA) becomes parallel to B. The correct position of the contours after their relative orientation is depicted with dashed lines. In the same fashion, all the adjacent pairs of contours were orientated in space.

The described vectors could be evaluated for each point of the 3D catheter trajectory, determining the relative orientation of each IVUS frame (Fig. 8). The point at which the plane of each frame intersected with the trajectory of the catheter was considered to be the control point. Initially, a reference axis was determined for the entire set of contours defined by an arbitrary selected reference point on the luminal contour of the first frame and its corresponding control point. Afterwards, the T, N and B vectors were evaluated at each control point and each pair of contours was rotated around the corresponding tangent vector at the plane defined by the normal and binormal vectors, until the reference axis was parallel to the binormal vector.